Homogeneous Bulk, Surface, and Edge Nucleation in Crystalline Nanodroplets

Jessica L. Carvalho and Kari Dalnoki-Veress*

Department of Physics and Astronomy and the Brockhouse Institute for Materials Research, McMaster University, Hamilton, Ontario, Canada

(Received 22 August 2010; revised manuscript received 19 October 2010; published 1 December 2010)

The birth of a crystal is initiated by a nucleus from which the crystal grows—a dust grain in a snowflake is a familiar example. These nuclei can be heterogeneous defects, like the dust grain, or homogeneous nuclei which are intrinsic to the material. Here we study homogeneous nucleation in nanoscale polymer droplets on a substrate which itself can be crystalline or amorphous. We observe a large difference in the nucleating ability of the substrate. Furthermore, the scaling dependence of nucleation on the size of the droplets proves that the birth of the crystalline state can be directed to originate predominantly within the bulk, at the substrate surface, or at the droplets' edge, depending on how we tune the substrate.

DOI: 10.1103/PhysRevLett.105.237801 PACS numbers: 61.41.+e, 64.60.Q−, 81.10.−h

Much debate exists within the community as to how polymers transition from an entangled melt of long-chain molecules to the initial crystal nucleus from which the crystalline state grows. Many ideas have been put forth, ranging from the classical nucleation and growth theories [1] to ideas involving a preordered mesomorphic precursor to the fully crystalline state [2]. Elucidating this earliest stage of crystal formation is fundamental to the study of crystallization in general and is investigated in a broad range of materials including model liquids [3], proteins [4], water [5], and colloids [6]. The ability to tune nucleation offers tremendous opportunity for adjusting material properties [7].

Extracting information about nucleation is complicated by the fact that the crystallization rate convolves crystal nucleation and crystal growth. Compounding this challenge is the prevalence of nucleation from defects in bulk samples. Thus, in recent years, researchers have looked to confining geometries as a means to isolate nucleation. One particular advantage confinement offers is the possibility for defect-free nucleation: if the material is subdivided into more small compartments than the number of defects in the system, then the ability to study *intrinsic* homogeneous nucleation rather than *defect driven* heterogeneous nucleation becomes possible. This concept dates back to pioneering work on phase-separated droplets of metals and organic systems [8–10], and more recently has been applied to a number of systems including phase-separated block copolymers [11–15], thin extruded films [7], solution grown crystals [16], alumina nanopores [17], and dewetted polymer droplets [18–20].

From the familiar example of snowflakes nucleating from a dust grain, it should not be surprising that interfaces play an important role in crystal nucleation. Simulations of nanosized droplets, similar to those formed through the dewetting process, found strong interface effects on the orientation of crystalline structures [20]. A clear example of a substrate affecting crystallization is that of epitaxy, where a particular crystalline orientation is induced by the substrate [21]. It is to be expected that through understanding the effects of epitaxy on nucleation and growth, insight into the mechanisms underlying crystallization can be gained.

We have previously studied nucleation using dewetted droplets ranging in size from ~ 10 μm to ~ 10 nm [18,19]. Thin films of polyethylene oxide (PEO) were dewetted from a smooth atactic polystyrene (PS) film; here the PEO and PS are analogous to water droplets forming on a waxy leaf. These samples contain many isolated PEO droplets which act as independent crystallization experiments. In particular, there is a separation of time scales making it possible to investigate nucleation independently from growth: as soon as a droplet forms a crystal nucleus, the entire droplet rapidly becomes crystalline. Thus, the crystallization of a single droplet is a direct probe of the nucleation event. Exploiting the idea that by subdividing the crystallizable material into tiny droplets that well outnumber the defects, we were able to systematically distinguish between heterogeneous and homogeneous nucleation and show that the homogeneous nucleation rate depended on the volume of a droplet [18,19]. Simply put, a droplet with twice the volume had twice the probability of nucleation.

Here we investigate the role of the interface in inducing crystal nucleation by using isotactic polystyrene (*i*-PS) as a substrate for PEO droplets, rather than smooth amorphous atactic PS [18,19]. Because of the regular stereochemistry of the phenyl side group, *i*-PS is capable of crystallizing. The ease with which the *i*-PS substrate can be prepared in either the crystal or amorphous state, simply by changing the thermal treatment, makes this an ideal model system for investigating interface effects. Thin films of PEO can then be dewetted producing droplets on either smooth amorphous *i*-PS (*ai*-PS) or rough crystalline *i*-PS (*ci*-PS) (see Fig. 1). While the chemical makeup of the amorphous and crystal *i*-PS films is identical, the substrate landscape in contact with the PEO droplets is vastly different, enabling a direct probe of the effect of the substrate on nucleation.

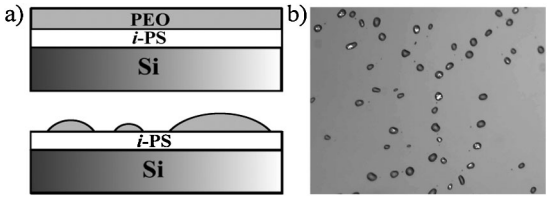

FIG. 1. (a) Schematic diagram of the sample geometry. *i*-PS film is prepared in the crystalline (*ci*-PS) or amorphous (*ai*-PS) state. Droplets of PEO are formed after the as-prepared sample (top) is allowed to dewet (bottom). (b) Optical microscopy image (width 400 μm) of a typical sample showing the dewetted droplets. Crystalline droplets appear bright.

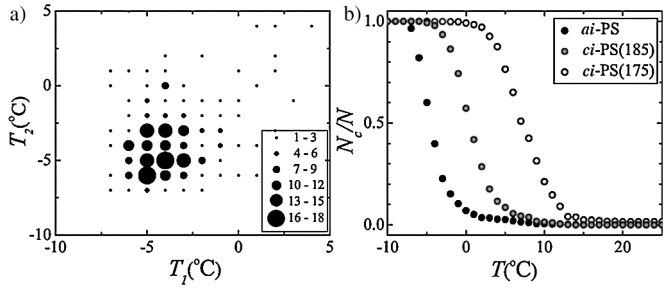

FIG. 2. (a) Typical correlation plot of the temperature at which a drop crystallizes in subsequent cooling runs. The PEO droplets on an amorphous *i*-PS substrate ranged in base radius from 3.5 to 7.5 μm, and were cooled from the melt at 1 °C/ min . (b) The fraction of crystallized droplets upon cooling for three types of substrates.

Thick *i*-PS films ($h > 400$ nm) were spin cast from cyclohexanone solutions onto clean Si substrates (molecular weight $M_w = 400$ kg/mol). All polymer used in this study was obtained from Polymer Source Inc., Canada. The *i*-PS films were annealed at 250 °C in vacuum (10^{-6} Torr), above the melting temperature for *i*-PS ($T_m \sim 240$ °C) for 5 min. To prepare *ai*-PS substrates, films were subsequently quenched to 135 °C and annealed for 2 h to further remove residual stresses, followed by a quench to room temperature. To prepare *ci*-PS substrates, films were quenched to either 175 °C or 185 °C following the 250 °C anneal, and held at this temperature for ~3 days, after which the films were fully covered with large crystal spherulites. These substrates will be distinguished as *ci*-PS(175) and *ci*-PS(185). Spherulites grown at different temperatures experience different crystal growth rates, affecting the degree of crystallinity and the roughness of the crystallized film [2]. Atomic force microscopy (AFM) was used to characterize the rms surface roughness of the different surfaces. The *ci*-PS(175) and *ci*-PS(185) substrates had a roughness of 12 ± 3 and 8 ± 1 nm, while the *ai*-PS surface was smooth, 0.7 ± 0.1 nm. We note that the roughness was obtained away from the boundary between two spherulites on the *ci*-PS substrate. Likewise, because we wanted to investigate nucleation of PEO droplets on the crystalline *i*-PS surfaces, droplets on the boundary were not included in the measurements. After preparation of the *i*-PS films, the samples were kept frozen below the glass transition of *i*-PS ($T_g \sim 100$ °C) to ensure there were no further changes. Films of PEO ($M_w = 27.2$ kg/mol and polydispersity index $M_w/M_n = 1.09$), with thickness $h \sim 70$ nm, were spin cast out of acetonitrile solutions onto the prepared *i*-PS substrates. These layered films were annealed at 80 °C in vacuum for ~4 days to allow the PEO films to dewet on the unfavorable *i*-PS surface as shown in Fig. 1. Three sets of samples were obtained: small, isolated droplets of PEO a few micrometers in radius and a few hundred nanometers tall, on *ai*-PS, *ci*-PS(175), and *ci*-PS(185). Samples were transferred to an optical microscope heating stage (Linkam, UK) flushed with argon for the crystallization experiments. Crystallization was followed with optical microscopy under nearly crossed polarizers [see Fig. 1(b)] [18]. One of the advantages of using small dewetted droplets is that, regardless of size, the droplets have the same contact angle. Thus, knowing the radius of the base of the droplets from optical microscopy R and the contact angle θ, the volume of each droplet is obtained [22]. AFM was used to determine that the contact angle was $17 \pm 3°$ for all three substrate preparations.

We have shown that correlation analysis is useful to differentiate homogeneous from heterogeneous nucleation [18]. In such experiments, the temperature at which a droplet crystallizes during a cooling run is plotted as a function of the crystallization temperature in an identical subsequent run. Data for the two nucleation mechanisms look qualitatively different on such correlation plots. A heterogeneity in a droplet affects the nucleation temperature the same way in subsequent runs: a specific droplet is more likely to form a crystal at the same temperature in both runs. However, different heterogeneities will result in varying nucleating temperatures, resulting in correlation data loosely scattered along a slope of 1 [18]. Since homogeneous nucleation is intrinsic to the system studied, two droplets with the same volume of material have the same chance of forming a nucleus at any given temperature. A typical correlation plot for the homogeneous mechanism is symmetric in nature, peaking where the nucleation rate is largest. A correlation plot for PEO droplets on the *ai*-PS substrate is shown in Fig. 2(a). The correlation plot shows a symmetric distribution peaked around −4.5 °C that is characteristic of the homogeneous mechanism, in full agreement with previous results for PEO drops on amorphous *atactic* PS substrates [18]. In the following, all the data presented deal with the population of homogeneously nucleated droplets. In Fig. 2(b) is shown a histogram of the number of nucleation events upon cooling for all three substrates. While the *ai*-PS substrate peaks at −4.5 °C, the two crystalline *i*-PS substrates show dramatically higher nucleation temperatures. In particular, we see enhancements in nucleation of about 6 °C and 12 °C for the drops on *ci*-PS(185) and *ci*-PS(175) substrates. Given the exponential dependence of nucleation rate on temperature [2], this represents a significant change in the activation barrier to nucleation. Differences in the barrier to nucleation are correlated to the roughness of the

substrate. The amorphous substrate is extremely uniform, while the *ci*-PS substrates represent very rough, nonuniform terrain, as evidenced by the large surface roughness values. This correlation is further supported by the fact that the *ci*-PS(175) film has a larger measured surface roughness and shows a higher nucleation temperature than the *ci*-PS(185) film.

Having established that merely changing the substrate topology from amorphous to crystalline has a significant effect on the nucleation temperature, the second aim of this study is to establish how substrate properties affect the scaling dependence of the nucleation probability on the size of droplets. Isothermal experiments were performed by quenching from 80 °C to the desired crystallization temperature T_c. For each substrate, T_c was chosen based on where the nucleation rate began to peak in Fig. 2(b) ($T_c = -2$ °C, 4 °C, and 10 °C). Assuming an ensemble of equally sized droplets, the rate of change in the amorphous fraction of droplets can be written as [18]

$$\frac{d}{dt}\left(\frac{N_a}{N}\right) = -P\left(\frac{N_a}{N}\right) = -\frac{1}{\tau}\left(\frac{N_a}{N}\right), \quad (1)$$

where N_a is the number of amorphous droplets, P is the probability per unit time of having a nucleation event, and τ is the time constant associated with nucleation events. Thus, $N_a/N = \exp(-t/\tau)$, and plots of the logarithm of the amorphous fraction of droplets as a function of time yield a linear relationship. The crystalline substrates are rough and the surface experienced by different droplets is not equivalent. As a result, upon cooling there is a population of droplets that nucleate at higher temperatures either because of heterogeneous nucleation or because the variations in the substrate result in a range of activation barriers to nucleation. Regardless, here we are concerned with the homogeneous population of droplets which elucidate the activation barrier that is intrinsic to the substrate-droplet system. It is this population that has the highest activation barrier to nucleation and nucleates at the lowest temperatures in cooling experiments, or nucleates last in isothermal experiments. Correlation experiments of the type shown in Fig. 2(a)were carried out to directly verify that the homogeneously nucleating droplet population was indeed the population that nucleated at later times in isothermal experiments.

In Figs. 3(a)–3(c) is shown the logarithm of the fraction of droplets remaining in the amorphous state as a function of time for isothermal crystallization for all three substrates. In accordance with Eq. (1), the data have been binned according to droplet size. The population of droplets nucleating after 400 s was considered for the two *ci*-PS substrates to guarantee that only homogeneous nucleation is represented. The slope of the best fit straight line to the data is $-1/\tau$ for each bin of droplet size, and this slope depends on the size of the droplet (i.e., a larger droplet is more likely to nucleate a crystal). We write $\tau \sim R^{-n}$, where R is the average radius of the droplet's base area, as measured by optical microscopy for a particular bin of droplets. There exist 3 physically meaningful possibilities for n: (1) If $n \sim 3$, then the system exhibits a volume dependent nucleation rate. It is this bulk nucleation that has been shown to be the case for PEO droplets on atactic PS surfaces [18]. (2) If $n \sim 2$, then nucleation is dependent on the surface area of the droplet and induced by the interaction of the droplet with the substrate. (3) If $n \sim 1$, then the nucleation scales with the linear dimension of the droplet. Specifically, since the only relevant linear dimension is the three-phase contact line of the droplet, the nucleation must be induced at the edge of the droplet. The scaling of τ with droplet length scale R is shown in Fig. 3(d) for each of the different *i*-PS substrates. As might have been expected, the *ai*-PS substrate shows a volume dependent nucleation rate, with $n \sim 3$, in agreement with our previous results on atactic PS [18]. Crystal nucleation is occurring within the bulk volume of the droplets when supported on an amorphous *i*-PS substrate. However, the scaling behavior for the two *ci*-PS films shows a remarkably different scaling not previously seen. The *ci*-PS(185) substrate data are consistent with $n \sim 2$. Thus, the crystal nuclei form predominantly at the surface of the PEO droplet in contact with the substrate. Even more surprising is the result for the *ci*-PS(175) substrate, which shows a line dependent nucleation rate, $n \sim 1$. This suggests that the crystal nuclei form predominantly on the contact line between the PEO droplet and the *ci*-PS(175) substrate. On

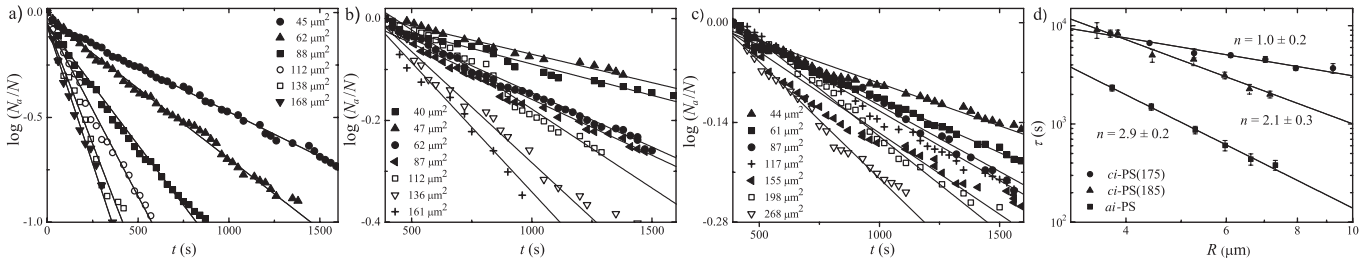

FIG. 3. (a)–(c) Logarithm of the amorphous fraction of droplets as a function of time for isothermal crystallization. The data are binned according to base area of droplets supported on the *ai*-PS substrate, *ci*-PS(185) substrate, and *ci*-PS(175) substrates, respectively. (d) Logarithmic plot of the time constant for homogeneous nucleation as a function of the radius of the base of the droplets obtained from (a)–(c). The differences in scaling indicate that bulk, surface, and line nucleation are observed. Since each sample type is crystallized at a different temperature, there is no significance to the crossing of the lines.

closer examination of the droplets on the *ci*-PS(175) substrate with AFM, nuclei originating at the contact line could clearly be seen for *every* droplet examined, confirming independently that $\tau \sim R^{-1}$. Examples of such droplets are shown in Fig. 4. The *ai*-PS and the *ci*-PS(185) substrates showed a variety of nucleation locations.

Through the use of PEO droplets on an *i*-PS substrate, we have shown that the nucleation properties are significantly affected by the properties of the substrate. The ease with which the *i*-PS substrate can be prepared in either the amorphous or crystalline state makes this an ideal system to compare nucleating ability of a smooth amorphous and a rough crystalline substrate. Given that the chemical makeup is identical in both cases, any enhancement in nucleating ability must be attributed to the physical characteristics of the substrate itself. We have shown a remarkable increase in the homogeneous nucleation temperature for the crystalline substrate by $\sim 12\,^{\circ}\mathrm{C}$ compared to that of the amorphous case. A crystalline substrate has a large range of important length scales from the molecular to mesoscopic. Which of these length scales is most influential to nucleation is not yet clear. Damman and co-workers [21] investigated rubbed crystal and amorphous substrates to determine if molecular epitaxy or surface topography played a greater role in the crystal growth of a small molecule system. While they found molecular order to be more important than mesoscopic roughness, it is difficult to say whether the same holds for polymers. Thus an interesting question remains: Is the enhancement in nucleation driven by a truly epitaxial mechanism or is it simply topography related? The process by which the droplets are formed may offer some insight into the origin of this nucleation control. As the PEO film dewets, the molecules flow. The presence of a rough, corrugated surface during flow is likely to contribute to enhanced chain alignment which may lower the activation barrier to nucleation. Chain alignment may be further enhanced by pinning molecules at the contact line. Since the droplets have been annealed for several days, it is reasonable to assume that there is no appreciable flow. However, the chains may be trapped in shear-aligned metastable conformations at the substrate due to the complex nature of the energy landscape induced by the roughness. Such speculation is in agreement with experiments by Jradi and co-workers [23], who observed enhanced nucleation in polymer films where the chains had been oriented through rubbing. We suspect that the origin of the nucleation enhancement is a property of the long-chain nature, and high susceptibility, of polymers. Furthermore, in contrast with the simple volume dependent nucleation probability found in droplets on an amorphous substrate, we have shown that the nucleation probability changes from being volume, to surface, to line dependent by tuning the substrate. Thus, changes in the substrate-droplet interface properties result in nucleation occurring within the *bulk* of the droplet, the *surface* of the droplet, or the three-phase contact *line* of the droplet.

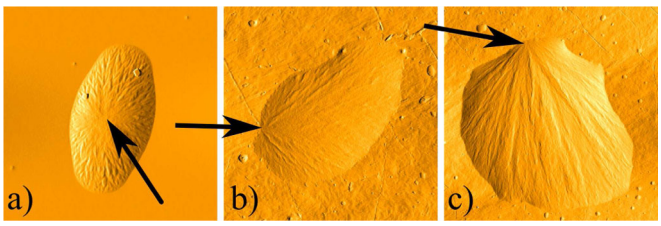

FIG. 4 (color online). AFM images (error signal) of crystalline PEO droplets on *i*-PS substrates (width $\sim 8\ \mu$m). (a) Droplet on *ai*-PS substrate, with the nucleus (arrow) visible at the center. (b),(c) Droplets on *ci*-PS(175) substrate. In both cases the nucleus originates at the contact line.

We thank Dr. Michael Massa and Professor Günter Reiter for valuable discussions. Financial support by NSERC of Canada is gratefully acknowledged.

*dalnoki@mcmaster.ca

[1] B. Lotz, Eur. Phys. J. E **3**, 185 (2000).
[2] G. Strobl, *The Physics of Polymers: Concepts for Understanding Their Structures and Behaviour* (Springer-Verlag, Berlin, 2007).
[3] D. Moroni, P. Ten Wolde, and P. Bolhuis, Phys. Rev. Lett. **94**, 235703 (2005).
[4] A. M. Streets and S. R. Quake, Phys. Rev. Lett. **104**, 178102 (2010).
[5] A. Michaelides and K. Morgenstern, Nature Mater. **6**, 597 (2007).
[6] A. Cacciuto, S. Auer, and D. Frenkel, Nature (London) **428**, 404 (2004).
[7] H. Wang *et al.*, Science **323**, 757 (2009).
[8] B. Vonnegut, J. Colloid Sci. **3**, 563 (1948).
[9] R. Cormia, F. Price, and D. Turnbull, J. Chem. Phys. **37**, 1333 (1962).
[10] J. Koutsky, A. Walton, and E. Baer, Appl. Phys. **38**, 1832 (1967).
[11] Y.-L. Loo, R. A. Register, and A. J. Ryan, Phys. Rev. Lett. **84**, 4120 (2000).
[12] G. Reiter *et al.*, Phys. Rev. Lett. **87**, 226101 (2001).
[13] A. Lorenzo *et al.*, Eur. Polym. J. **42**, 516 (2006).
[14] J. Carvalho, M. Massa, and K. Dalnoki-Veress, J. Polym. Sci., Part B: Polym. Phys. **44**, 3448 (2006).
[15] T. Cai *et al.*, Macromolecules **42**, 3381 (2009).
[16] M. Hsiao *et al.*, Macromolecules **41**, 4794 (2008).
[17] E. Woo *et al.*, Phys. Rev. Lett. **98**, 136103 (2007).
[18] M. V. Massa and K. Dalnoki-Veress, Phys. Rev. Lett. **92**, 255509 (2004).
[19] M. V. Massa, J. L. Carvalho, and K. Dalnoki-Veress, Phys. Rev. Lett. **97**, 247802 (2006).
[20] W. Hu *et al.*, Faraday Discuss. **143**, 129 (2009).
[21] P. Damman *et al.*, J. Am. Chem. Soc. **124**, 15166 (2002).
[22] This assumes spherical cap droplets, resulting in an error in the volume that is negligible for these experiments.
[23] K. Jradi *et al.*, Eur. Phys. J. E **29**, 383 (2009).